Cross-Talk between Nucleotide Excision and Homologous Recombination DNA Repair Pathways in the Mechanism of Action of Antitumor Trabectedin

Ana B. Herrero,[1] Cristina Martín-Castellanos,[1] Esther Marco,[2] Federico Gago,[2] and Sergio Moreno[1]

[1]Instituto de Biología Molecular y Celular del Cáncer, Consejo Superior de Investigaciones Científicas/Universidad de Salamanca, Campus Miguel de Unamuno, Salamanca and [2]Departamento de Farmacología, Universidad de Alcalá, Alcalá de Henares, Madrid, Spain

Abstract

Trabectedin (Yondelis) is a potent antitumor drug that has the unique characteristic of killing cells by poisoning the DNA nucleotide excision repair (NER) machinery. The basis for the NER-dependent toxicity has not yet been elucidated but it has been proposed as the major determinant for the drug's cytotoxicity. To study the *in vivo* mode of action of trabectedin and to explore the role of NER in its cytotoxicity, we used the fission yeast *Schizosaccharomyces pombe* as a model system. Treatment of *S. pombe* wild-type cells with trabectedin led to cell cycle delay and activation of the DNA damage checkpoint, indicating that the drug causes DNA damage *in vivo*. DNA damage induced by the drug is mostly caused by the NER protein, Rad13 (the fission yeast orthologue to human XPG), and is mainly repaired by homologous recombination. By constructing different *rad13* mutants, we show that the DNA damage induced by trabectedin depends on a 46–amino acid region of Rad13 that is homologous to a DNA-binding region of human nuclease FEN-1. More specifically, an arginine residue in Rad13 (Arg961), conserved in FEN1 (Arg314), was found to be crucial for the drug's cytotoxicity. These results lead us to propose a model for the action of trabectedin in eukaryotic cells in which the formation of a Rad13/DNA-trabectedin ternary complex, stabilized by Arg961, results in cell death. (Cancer Res 2006; 66(16): 8155-62)

Introduction

Trabectedin (Yondelis) is a novel antitumor agent originally isolated from the Caribbean marine tunicate, *Ecteinascidia turbinata*, which was selected for clinical investigation due to its potent cytotoxic activity against a variety of tumor cell lines *in vitro* and human tumor xenografts *in vivo* (1). Currently, trabectedin is undergoing phase II/III clinical trials both in Europe and the U.S., with promising results for the treatment of soft tissue sarcomas, and breast and ovarian cancers (2–4).

Despite its advanced stage in clinical investigation, the precise mechanism of action of trabectedin remains poorly understood. DNA seems to be an important target because the drug has been shown to form, *in vitro*, covalent adducts with the N2 of guanines located in the DNA minor groove (5, 6). The most prominent characteristic that makes its mechanism of action unique as compared with classic DNA-binding antitumor drugs is the atypical response detected in cells affected in the DNA repair mechanism nucleotide excision repair (NER). Whereas all known DNA-interacting drugs are either more effective or equally effective in NER-proficient and NER-deficient cells, trabectedin has been shown to be less effective in NER-deficient cells (7, 8). A hypothesis to explain this particular behavior has been proposed; i.e., that the drug may interact with the NER machinery to induce lethal DNA strand breaks (9).

To gain some insight into the *in vivo* mechanism of action of trabectedin and to explore the contribution of the NER system in such a mechanism, we used the fission yeast, *Schizosaccharomyces pombe*, as a model organism. Using this yeast, we observed that trabectedin causes DNA damage *in vivo* because it activates the S phase and G_2-M DNA damage checkpoint responses. Moreover, cells deficient in homologous recombination repair (HRR) are extremely sensitive to the drug, indicating that trabectedin probably causes double-strand breaks (DSB). As also found in mammalian cells, NER mediates trabectedin's cytotoxicity in *S. pombe* cells. In particular, cells deficient in Rad13 (the fission yeast orthologue to human XPG) are less sensitive to the drug. By constructing different mutants in the Rad13 protein, we have shown that (*a*) the ability of Rad13 to produce single-strand breaks (SSB) is not required for trabectedin's cytotoxicity, and (*b*) that a short region in the COOH terminus of the protein is involved in NER-dependent cell killing. The involvement of NER in the formation of trabectedin-DNA lethal complexes and HRR in its resolution are discussed.

Materials and Methods

Drugs, strains, media, and growth conditions. Trabectedin was obtained from PharmaMar and prepared as a 1 mmol/L stock solution in ethanol that was kept at −20°C. Methyl methanesulfonate (MMS) was supplied by Fluka (Buchs, Switzerland) and 4-nitroquinoline 1-oxide (4NQO) was supplied by Sigma (St. Louis, MO). The *S. pombe* strains used in this study are listed in Table S1 (supplemental data). Standard *S. pombe* molecular genetic techniques and the media were used as described previously (10).

Spot assays for analyzing sensitivity to trabectedin and MMS. Yeast strains were grown in YES medium until they reached the exponential phase. Cells were harvested by centrifugation and resuspended in YES medium to an absorbance of 2 (OD_{595}), corresponding to 2×10^7 cells/mL. Five microliters of undiluted cell culture and 1/10 serial dilutions of each cell culture were spotted onto YES plates containing trabectedin (1-10 μmol/L), MMS (0.005-0.01%), or 4NQO (0.05 μg/mL).

Fluorescence-activated cell sorting analysis. Approximately 10^7 cells were spun down, fixed in 70% ethanol, and processed for flow cytometry

as described previously (10). A Becton Dickinson (Mountain View, CA) FACSCalibur was used. Cell size measurements were calculated with the forward-light scatter data of fluorescence-activated cell sorting (FACS), considering 100 as the size of the wild-type control.

4′,6-Diamidino-2-phenylindole staining and microscopy. Ethanol-fixed cells were rehydrated and stained with 4′,6-diamidino-2-phenylindole at a final concentration of 0.05 mg/mL. Pictures were taken with a Leica DM6000 B microscope, using a Hamamatsu ORCA-ER camera and Openlab 4.0.3 software.

Protein extracts and Western blots. About 3×10^8 cells growing in YES medium were collected and processed for total protein extraction, as described previously (10). For Chk1HA detection, 50 μg of total protein extract was run on an 8% SDS-PAGE gel, transferred to nitrocellulose, and incubated with anti-HA monoclonal antibodies, 12CA5 (0.16 μg/mL), for 2 hours at room temperature. Sheep anti-mouse antibodies conjugated to horseradish peroxidase (1/2,000; Amersham) were used as secondary antibodies in 40-minute incubations at room temperature. Protein extracts for Rad13HA detection were obtained by TCA precipitation, as described previously (11), and resuspended in 200 μL of Laemmli buffer. Aliquots (25 μL) of the extracts were run on a 7% SDS-PAGE gel and Western blotted as described above. The immunoblots were developed using Super Signal (Pierce, Rockford, IL).

For details regarding the cloning of *rad13* and construction of *rad13* mutants, as well as the construction, refinement, and molecular dynamics simulations of a Rad13/DNA-trabectedin ternary complex, see supplemental data.

Results

Trabectedin causes cell cycle arrest in G2-M in fission yeast. To assess whether trabectedin elicits DNA damage, we first looked at the phenotype induced by this drug in *S. pombe* wild-type cells. When fission yeast cells were grown on plates containing trabectedin, we observed two different phenotypes depending on the concentration of the drug. At low concentrations (5-25 μmol/L), the cells became elongated with a characteristic cell cycle arrest phenotype. At high concentrations (25-100 μmol/L), the cells became small and round, and stopped growth after a few divisions. The cell cycle arrest phenotype consisted of elongated cells with a 2C DNA content, suggesting a possible delay in either the G2-M transition or in mitosis (Fig. 1). Nuclear staining revealed that these cells arrested with an interphase nucleus (Fig. 1), indicating that the arrest was produced at G2-M. Further evidence of the G2-M arrest phenotype is presented in the supplemental data.

Trabectedin activates the intra-S phase and the G2-M DNA damage checkpoints. Because trabectedin is able to bind to DNA

Figure 1. Trabectedin causes a G2-M delay in *S. pombe*. Cell elongation induced by the drug (*left*). FACS analysis of a time course experiment of *S. pombe* treated with trabectedin (*right*). A homogenous 2C DNA-content population was observed.

in vitro (5, 6, 12), and causes a cell cycle delay in G2, it was reasonable to speculate that this drug was activating the G2-M DNA damage checkpoint. To test this possibility, we examined the sensitivity to trabectedin of a variety of checkpoint mutants in serial dilution experiments. First, we analyzed a set of mutants involved in the recognition of the DNA lesion: *rad1Δ*, *rad9Δ*, and *rad17Δ*, and a mutant involved in the transduction of the signal, *rad3Δ* (13). All of these mutants were hypersensitive to trabectedin (Fig. 2*A*), indicating that cells that are unable to activate the DNA damage checkpoint response are less tolerant to the drug. This hypersensitivity was observed even at 1 μmol/L of trabectedin, a concentration at which wild-type cells did not show any phenotype on plates.

Chk1 and Cds1 are two effector kinases activated by the sensors/transducer described above (14, 15). Cds1 is specific for the DNA damage induced during S phase, and Chk1 is activated in response to DNA damage induced in G2. *chk1Δ* cells were also more sensitive than the wild-type to trabectedin treatment. Cell survival was reduced and cells barely elongated in the presence of the drug (Fig. 2*A* and *B*). Surprisingly, we observed increased resistance to trabectedin in *cds1Δ* cells as compared with wild-type cells (Fig. 2*A*). The same behavior has been reported for *cds1* mutant cells treated with the bifunctional (alkylating and interstrand cross-linking) antitumor agents, nitrogen mustard and mitomycin C (16), possibly reflecting the fact that the delay in S phase and the attempt to repair the DNA damage caused by these drugs may be detrimental for cell survival. To study the possible effect of trabectedin during S phase, we synchronized cells in G1 by nitrogen depletion and allowed them to reenter the cell cycle with or without the drug. Wild-type cells treated with trabectedin entered S phase at the same time as untreated cells (Fig. 2*C*, 2-3 hours). However, they were delayed in their progression through S phase (Fig. 2*C*, arrows). This delay was specifically abolished in a *cds1Δ* strain but not in a *chk1Δ* strain (Fig. 2*C*), corroborating the idea that trabectedin produces lesions in the DNA (9, 17), and showing that it elicits DNA damage response in both S and G2 phases.

The DNA damage response elicited by trabectedin recruits proteins from both the NER and homologous recombination machineries. In order to understand the type of DNA damage response evoked by the drug, we tested the sensitivity to trabectedin of a variety of mutants in different DNA damage repair pathways [NER, UV excision repair and homologous recombination (HR) repair]. We used the following NER mutants: *rph14Δ* (an orthologue to the mammalian XPA and likely involved in lesion recognition), *swi10Δ* and *rad16Δ* [orthologues to mammalian ERCC1 and XPF, endonucleases involved in single-stranded DNA (ssDNA) incision 5′ to the DNA lesion], and *rad13Δ* (an endonuclease orthologue to mammalian XPG that is involved in ssDNA incision 3′ to the lesion; ref. 18). In the UV excision repair (UVER) pathway, we used mutant strains, *uve1Δ* and *rad2Δ*, which lack ssDNA 5′ and 3′ endonucleases for this repair pathway, respectively (19). Finally, in the HRR pathway, the *rad51Δ*, *rad22Δ*, and *rad54Δ* strains were used. Rad51 is required in the initial steps of HRR for homologous pairing and DNA strand exchange (20). Rad22 is the fission yeast counterpart of the mammalian DNA-binding protein, Rad52, that helps to load Rad51 onto the recombination site and also promotes annealing of complementary ssDNA (21). Rad54 is a dsDNA-stimulated ATPase homologue of mammalian Rad54 (22) that is involved in DNA remodeling and whose activity is stimulated by Rad51 (23).
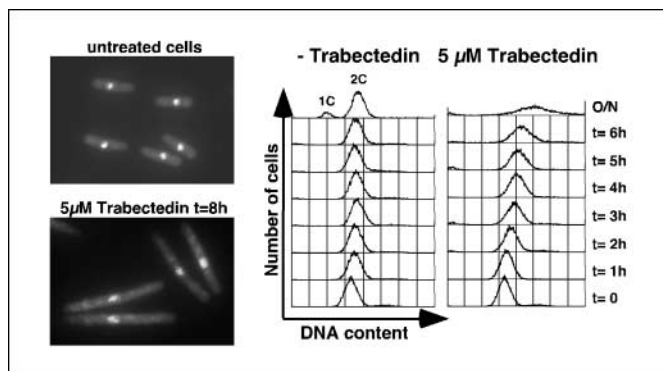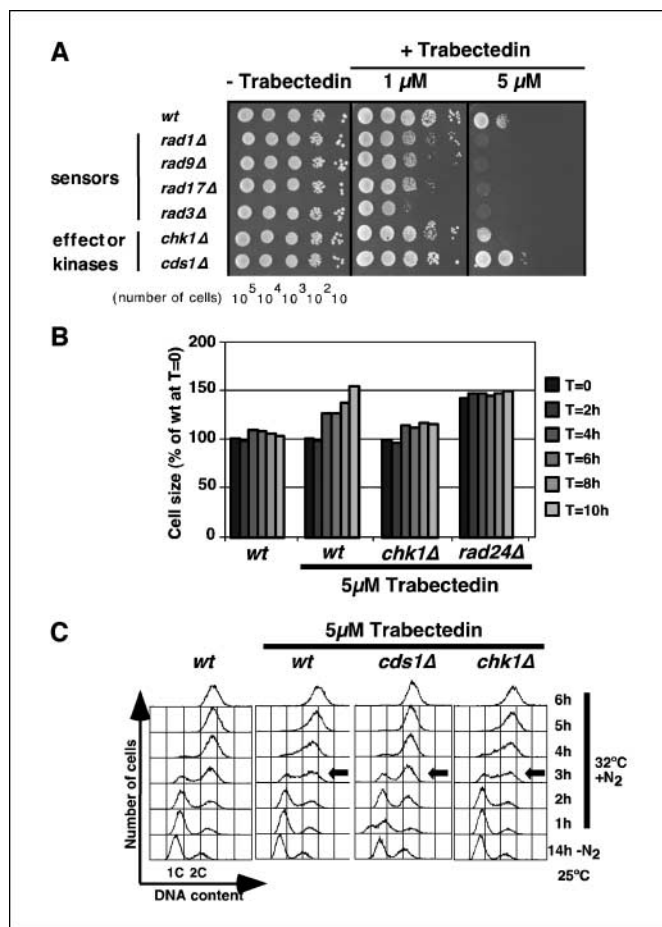
Figure 2. Trabectedin activates the DNA damage response. *A,* sensitivity to trabectedin of different mutants affecting sensors, transducers, and effectors of the DNA damage checkpoint response. Except for *cds1Δ*, all these mutants are more sensitive to the drug than control wild-type cells. *B,* cell size of the indicated strains during a time course experiment. Whereas wild-type cells elongate in response to trabectedin treatment, *chk1Δ* and *rad24Δ* do not. *C,* FACS analysis of the kinetics of S phase progression in the presence of trabectedin. Trabectedin causes an S phase delay (*arrows*) that is overcome in a *cds1Δ* strain but not in a *chk1Δ* strain.

Strains disrupted for *rad2* or *uve1*, both required for UVER, were as sensitive to the drug as wild-type cells (Fig. 3A). However, mutants impaired in HRR (*rad51Δ* and *rad54Δ*) were extremely sensitive to trabectedin (Fig. 3A). They were hypersensitive even at 1 μmol/L of trabectedin, a concentration at which wild-type cells do not show any phenotype on plates. The hypersensitivity of these mutants to the drug suggests that trabectedin might give rise to DSB. In striking contrast, mutants in genes involved in NER, except *rhp14Δ*, were more resistant to the drug. In particular, the *rad13Δ* mutant (lacking the *XPG* orthologue) was the most resistant (Fig. 3A). Sensitivity to trabectedin was recovered when *rad13Δ* cells were transformed with a multicopy plasmid carrying the *rad13* gene (Fig. 3B). These effects were specific for trabectedin because they were not observed for MMS (Fig. 3B). Whereas the *rad13* deletion conferred resistance to trabectedin, *rad13* overexpression induced hypersensitivity to the drug (Fig. 3C). The decreased sensitivity of this particular NER mutant to trabectedin has also been reported in mammalian cells (9) and in *Saccharomyces cerevisiae* (17), and suggests that Rad13 (XPG) is somehow involved in generating the DNA damage signal elicited upon trabectedin treatment.

Trabectedin requires *rad13* to induce DNA damage and to activate the DNA damage checkpoint. The partial resistance of NER mutant cells to trabectedin indicates that it is more deleterious for drug-treated cells to have a functional *rad13* gene. Thus, Rad13 could be involved in generating the DNA damage and/or in checkpoint activation. To test this hypothesis, we first analyzed changes in cell size as an indication of the cell cycle delay induced by the drug during a time course experiment comparing wild-type and *rad13Δ* strains. *rad13Δ* mutant cells elongated much less and showed a better appearance under the microscope than trabectedin-treated wild-type cells, (Fig. 4A and B). This result indicates that the cell cycle delay induced by trabectedin is almost completely abolished when *rad13* is not present in the cell. We then measured the activation of the DNA damage checkpoint following the phosphorylation status of the Chk1 kinase. Chk1 phosphorylation was visualized by Western blot as a new band running above the unphosphorylated form when cells were treated with MMS for 3 hours (Fig. 4C). Deletion of *rad13* had no effect on
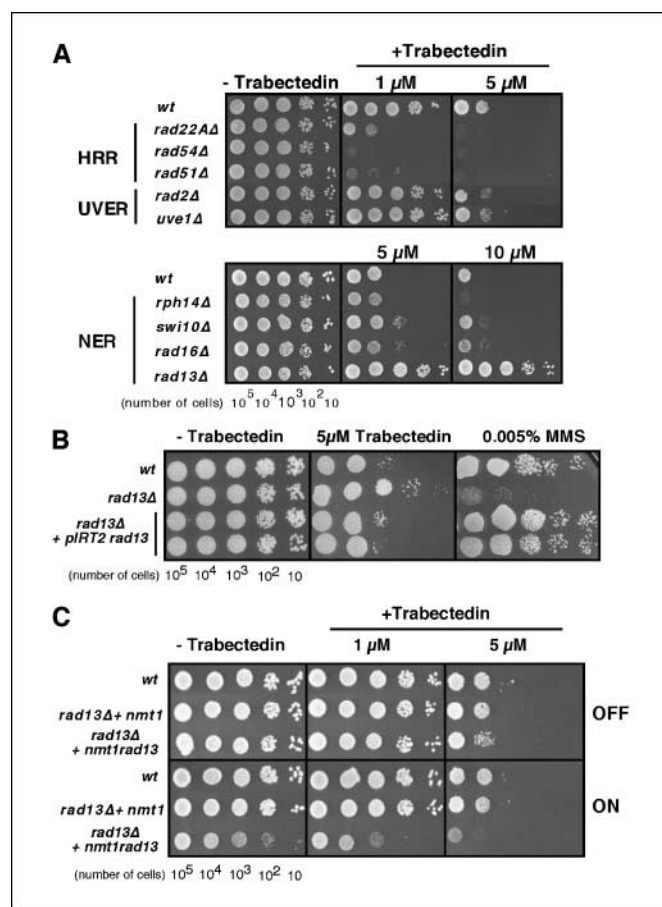

Figure 3. *A,* sensitivity to trabectedin of different mutants affected in DNA repair. Mutants affected in HRR, UVER, and NER. Note the extreme tolerance to trabectedin of *rad13Δ* cells (NER deficient) and compare this with the extreme sensitivity of HRR mutants. *B,* sensitivity to trabectedin of *rad13Δ* cells and the same cells transformed with a plasmid containing the *rad13* gene under the control of its own promoter. The resistance of *rad13Δ* to trabectedin is blocked when the production of Rad13 is restored in the transformed cells (*rad13Δ + pIRT2rad13,* two independent clones are shown). The same is true for the sensitivity to MMS of *rad13Δ* (MMS-containing plate). Note in this case that *rad13Δ* cells are more sensitive to MMS than control wild-type cells. *C,* sensitivity to trabectedin of *rad13Δ* expressing high levels of Rad13 under the thiamine-repressible promoter nmt1. Rad13 overexpression (*ON*) increases sensitivity to trabectedin. Compare *rad13Δ + nmt1* (empty vector) to *rad13Δ + nmt1rad13.*
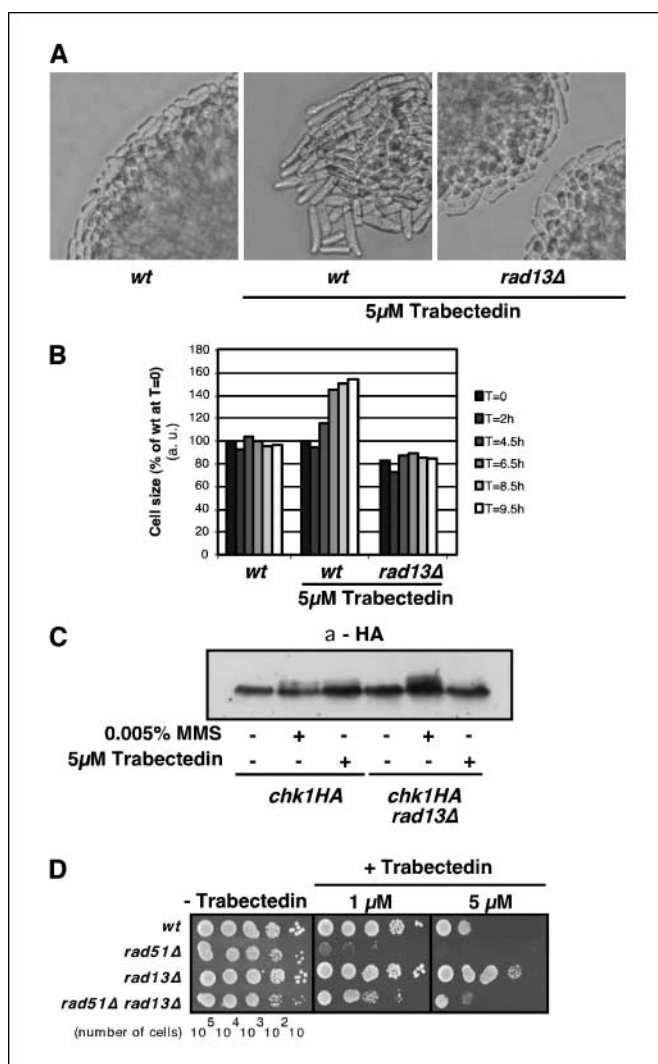
Figure 4. Reduction of DNA damage checkpoint response in *rad13Δ* cells. *A,* pictures of wild-type and *rad13Δ* cells treated with trabectedin, showing the block in elongation in *rad13Δ*. *B,* quantification of the elongation phenotype during a time course experiment. *C,* Western blot showing Chk1-HA mobility shift in response to MMS and trabectedin treatment in wild-type and *rad13Δ* strains. The mobility shift is reduced in *rad13Δ* cells treated with trabectedin, but not with MMS. *D,* the extreme sensitivity to trabectedin of *rad51Δ* cells is reduced in the *rad51Δ rad13Δ* double mutant.

the activation of Chk1 because the same mobility shift was detected when cells were treated with MMS for 3 hours (Fig. 4C, compare *lanes 2* and *5*). However, a reduction in Chk1 activation was observed in the *rad13Δ* mutant in the presence of trabectedin (Fig. 4C, compare *lanes 3* and *6*).

To further study the role of Rad13, we analyzed the sensitivity to trabectedin of the double mutant *rad51Δ rad13Δ*. If Rad13 is somehow involved in generating DNA damage in cells treated with the drug, deletion of *rad13* should suppress the hypersensitivity of *rad51Δ* mutant cells because the damage that Rad51 repairs is eliminated. *rad51Δ rad13Δ* double mutant cells were found to be more resistant to trabectedin than the single *rad51Δ* mutants (Fig. 4D). However, the double mutant was still more sensitive to the drug than the single *rad13Δ* (Fig. 4D). Similar to what happens in a wild-type background, the deletion of *rad13* abolished the cellular phenotypes (elongation and lysis) induced by trabectedin in

the *rad51Δ* background (data not shown). This result indicates that Rad13 is essential for the induction of DNA damage, although in its absence, there are still some DNA lesions that require repair by HR.

Trabectedin requires Rad13, but not its nuclease activity, to induce DNA damage. The NER 3′ endonucleases Rad13, human XPG, and *S. cerevisiae* Rad2 are members of a large nuclease family that also includes the structure-specific endonuclease-1 (FEN-1), an enzyme that specifically recognizes the 3′ DNA flap structure that has been proposed to exist during replication, repair, and recombination (24). All these proteins possess three conserved regions: two of them highly conserved at the NH$_2$ terminus (*N*) and the internal region (*I*), and a moderately conserved COOH-terminal region (*C*) (Fig. 5*A*). Different authors have shown that a mutation to alanine of a glutamate residue in the highly conserved sequence EAEA in region I completely abolishes the catalytic activity of XPG, Rad2, and FEN-1 (25, 26). Because it has been proposed that DNA damage induced by trabectedin in mammalian cells results from NER endonuclease activity, producing lethal SSBs (9), we decided to mutagenize the *S. pombe* Rad13E779 residue to alanine (equivalent to the human XPGE791A, Rad2E794A, and FEN-1E160A mutations) and analyze the effect of the mutation on sensitivity to trabectedin. The *rad13E779A* mutant allele was used to replace *rad13* in the fission yeast chromosome and the sensitivity to trabectedin was analyzed (Fig. 5*C*). In the same experiment, we also checked the sensitivity of this *S. pombe* strain to MMS. NER deletion mutants were more sensitive to MMS (Fig. 5*C*), as previously reported (27). The fact that the strain carrying the mutant version *rad13E779A* (Fig. 5*C, lane 3*) was more sensitive to both, MMS and 4NQO, a drug that mimics the effect of UV light, as compared with the wild-type strain (*lane 1*) indicated that the mutation of E779 was affecting the ability of Rad13 to excise in 3′, as expected. However, this mutation did not confer resistance to trabectedin (plates + trabectedin, *lane 3*) unlike the deletion of *rad13* (*lane 2*), indicating that the endonuclease activity of Rad13 is not required for the DNA damage induced by trabectedin. Moreover, we found that the E779A mutation increased the sensitivity of the cells to the drug. This observation suggests that the endonuclease activity of Rad13 could actually contribute to the repair of the DNA damage induced by trabectedin.

Rad13 COOH terminus is a target for trabectedin. Several lines of evidence have indicated that the COOH-terminal part of XPG exerts an endonuclease-independent function (28, 29); therefore, we decided to explore whether the COOH terminus of Rad13 was somehow contributing to trabectedin sensitivity. For this purpose, a *S. pombe* mutant strain with a Rad13 COOH-terminal truncation was constructed, and sensitivity to trabectedin was analyzed. Because XPG has been reported to contain in its COOH terminus nuclear localization signals (NLS) that mediate nuclear localization (30), and because NLSs also exist in FEN-1, Rad2, and Rad13 (Fig. 5*A*), we decided to delete most of the COOH-terminal domain of Rad13, except for a short region (amino acids 1,047-1,112) that contained the NLSs KRRR, RRRK and the bipartite signal RKTKLSTSLLKKPSKRR. We found that the *rad13CΔ* strain (Fig. 5*C, lane 4*) was as resistant to trabectedin as the *rad13* null mutant (Fig. 5*C, lane 2*), indicating that this part of the protein is essential for trabectedin cytotoxicity.

In order to identify which region within the COOH-terminal part of Rad13 was responsible for the phenotype exhibited by *rad13CΔ*, we searched for functional domains that had been previously characterized in this family of nucleases. This search gave us two possible candidates (Fig. 5*A*), (*a*) a domain previously described in

FEN-1 and XPG to bind proliferating cell nuclear antigen (PCNA), a ring-shaped homotrimeric protein that encircles DNA and acts as a "sliding clamp" which links the polymerase to the DNA template (31, 32), and (*b*) a domain reported in FEN-1 to form two α-helices involved in binding and recognizing double-stranded DNA associated with a 3′ flap, as observed in the X-ray crystal structure of a FEN-1/DNA complex (32). To analyze the contribution of each of these two domains, we constructed the following *S. pombe* strains: *rad13PΔ*, lacking amino acids 970 to 1000 of Rad13, which include the putative PCNA binding site, and *rad13DΔ*, lacking amino acids 925 to 969, encompassing the putative DNA binding domain (Fig. 5*A* and *B*). When the *rad13PΔ* mutants were assayed against trabectedin, we clearly observed that the presence of the mutated protein did not increase trabectedin resistance (Fig. 5*C, lane 5*). Moreover, as shown above for the *rad13E779A* strain, the expression of Rad13PΔ lead to a loss of endonuclease activity (detected as increased sensitivity to MMS and 4NQO as compared with the wild-type strain), which resulted in increased sensitivity to trabectedin as compared with the wild-type strain (Fig. 5*C, lane 1*). On the other hand, the *rad13DΔ* strain (Fig. 5*C, lane 6*) was found to be as resistant to trabectedin as the *rad13Δ* mutant strain. In conclusion, the PCNA binding region of Rad13 is dispensable,

whereas a short COOH-terminal region (amino acids 925-969) is essential for trabectedin-induced cytotoxicity.

Pinpointing a conserved arginine in Rad13 as an important residue for resistance to trabectedin. To understand the molecular basis through which the COOH-terminal region of Rad13 is involved in the mechanism of resistance to trabectedin, we built a model of Rad13, in complex with a double-stranded DNA molecule containing a 3′ flap, on the basis of its homology to FEN-1 (32). The model revealed that Arg961 from α15 in Rad13 occupies a position equivalent to that of Arg314 in FEN-1, which is the only residue that points toward the minor groove. Because trabectedin binds covalently to guanines in the DNA minor groove, we speculated that Arg961 might be interacting with the drug, thereby stabilizing a Rad13/DNA-trabectedin ternary complex. To test this hypothesis, the trabectedin molecule, which is composed of three fused tetrahydroisoquinoline rings (Fig. 6*A*), was incorporated into the Rad13/DNA complex, as described in Materials and Methods. A suitable location for the drug was found three bases upstream from the flap. In this ternary complex (Fig. 6*B*), we observed that a hydrogen bond could indeed be formed between Arg961 and subunit C of trabectedin, and that it was later maintained during the ensuing molecular dynamics simulation in aqueous solution.

Figure 5. Sensitivity to trabectedin of different *rad13* mutants. *A*, schematic representation of FEN-1, Rad2, XPG, and Rad13 proteins. The DNA-binding regions (*D*) and PCNA-binding regions (*P*) are expanded to show homology. The boxed residues correspond to conserved amino acids: arginine (*R*), in FEN-1 and Rad13, and lysine (*K*) in Rad2 and XPG. *B*, schematic of mutations in the Rad13 protein. *C*, sensitivity to trabectedin of different *S. pombe* strains. *D*, Western blot showing the expression of HA-tagged versions of Rad13 wild-type, point mutants and COOH-terminal deleted proteins.
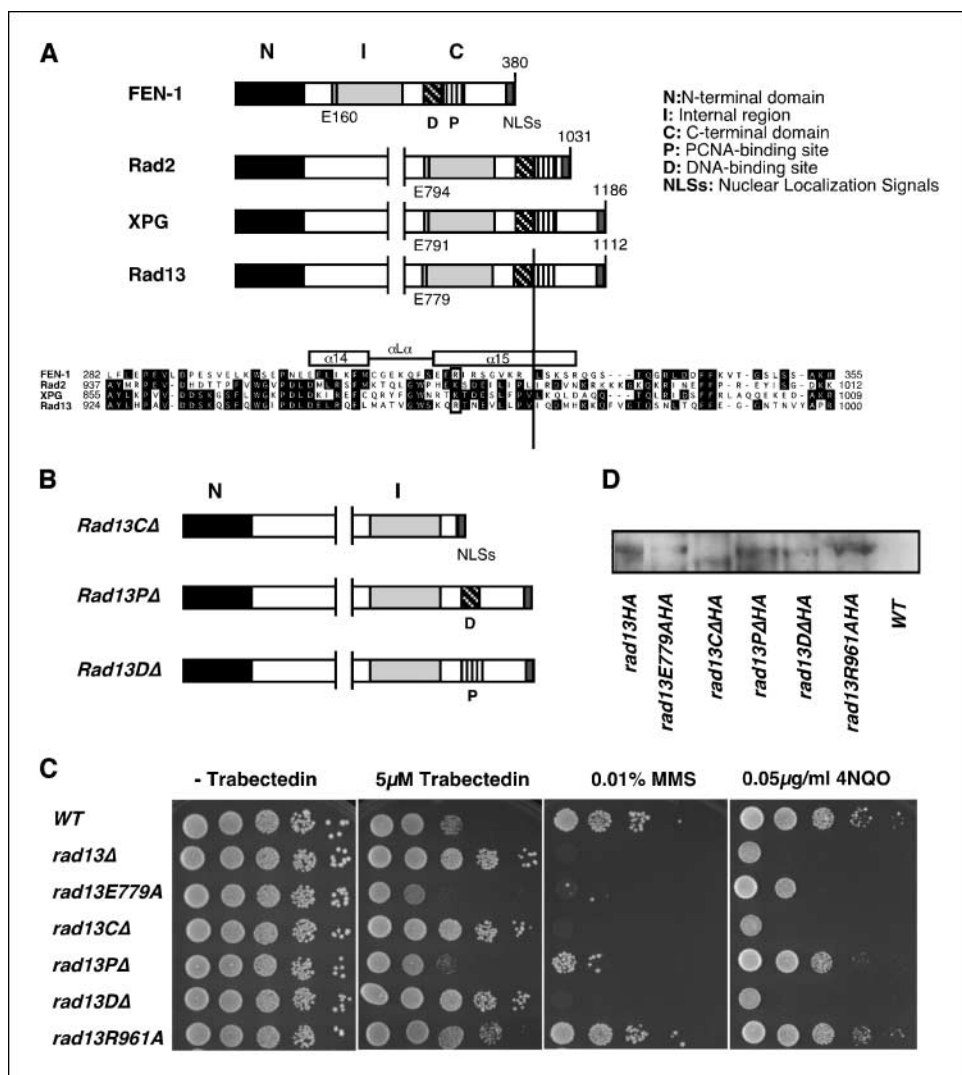
In the equilibrated complex, Rad13 is seen to recognize the widened minor groove of the DNA molecule and simultaneously interact with the guanine-bonded drug. One side of the C subunit of trabectedin makes extensive van der Waals contacts with the sugar-phosphate backbone of the two nucleotides downstream from the covalently bonded nucleotide, whereas the other side is exposed to the solvent and remains close to the guanidinium group of Arg961. Hence, it seems feasible that the side chain of this amino acid would establish good hydrogen-bonding interactions with both the hydroxyl and methoxy oxygens present in this subunit, which protrudes out of the minor groove, thereby contributing to ternary complex stabilization.

To analyze the effect of the Arg961 residue on the cytotoxicity exerted by trabectedin, a mutant strain carrying the R961A mutation was created, and sensitivity to trabectedin and MMS was analyzed. The fact that the *rad13R961A* strain was found to be as resistant to MMS and 4NQO (Fig. 5C, *lane 7*) as the wild-type strain (Fig. 5C, *lane 1*) clearly indicated that the mutated protein is functional and does not affect the efficiency of DNA repair. However, we found that this point mutation conferred resistance to trabectedin (Fig. 5C, plates + trabectedin, *lane 7*), indicating that the drug requires this particular arginine residue of Rad13 (Arg961) to induce its cytotoxic effect.
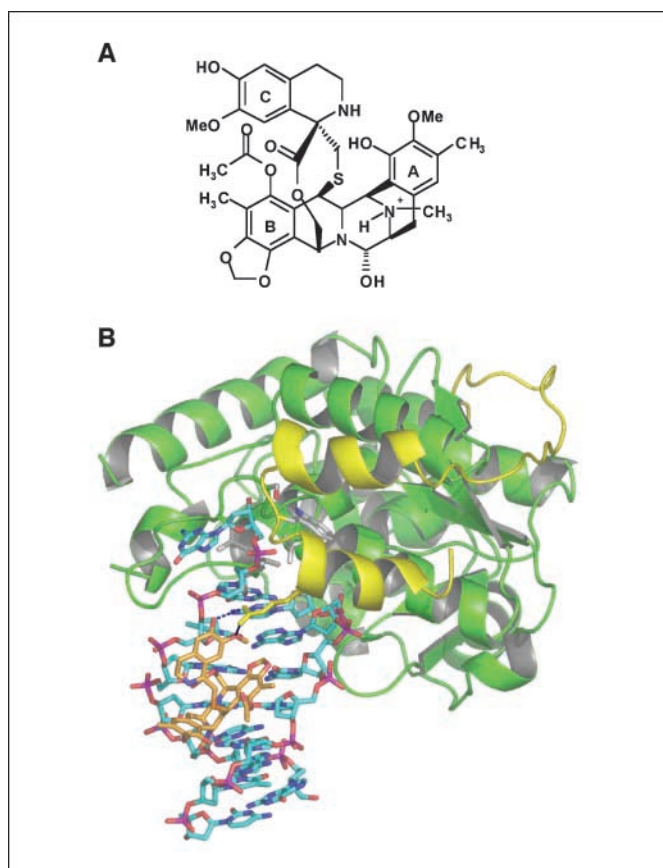

Figure 6. Model for Rad13-DNA-trabectidin interaction. *A,* chemical structure of trabectedin with three main subunits (*A*, *B*, and *C*). *B,* schematic representation of the modeled Rad13/DNA-trabectedin ternary complex. Trabectedin (C atoms, *orange*) is covalently bonded to a guanine in the DNA molecule (C atoms, *cyan*). *Green,* the N-region and I-region domains of Rad13; *yellow,* helices α14 and α15 and the connecting loop. The side chain of Arg961 (*yellow sticks*) establishes two good hydrogen bonds (*dots*) with the two oxygens present in subunit C of trabectedin. Hydrophobic residues making up the wedge (*sticks*) with C atoms (*gray*).

To verify that the Rad13 mutant proteins had been expressed, we constructed COOH-terminal HA-tagged versions of Rad13 wild-type, point mutants, and COOH-terminal deleted proteins. We then analyzed the expression of these proteins by Western blotting and their functionality by assaying the sensitivity of the strains to trabectedin and MMS (Supplemental Fig. S2). HA-tagged proteins were detected in all the strains constructed (Fig. 5D), and the strains behaved like their non-tagged counterparts in terms of sensitivity to both trabectedin and MMS.

Discussion

In the present study, we took advantage of *S. pombe* genetics to clarify important aspects regarding the mechanisms of action of the antitumor drug trabectedin. Here, we report that trabectedin activates the G_2-M and S phase DNA damage checkpoints mediated, respectively, by the effector kinases Chk1 (Fig. 2A and B) and Cds1 (Fig. 2C), in good agreement with the S phase delay and G_2-M block reported in human cells (8, 33–35). Furthermore, treatment of *S. pombe* cells with trabectedin also produces concentration-dependent phenotypes: at low concentrations, the drug induced cell cycle delay in S phase and a G_2-M block, whereas at higher concentrations, the cells treated with the drug stopped growing and died (Figs. 1 and 2A; data not shown). Similar cytostatic (at low doses) and proapoptotic (at high doses) effects have been described for cancer cells treated with trabectedin (34).

Role of NER in trabectedin cytotoxicity. NER proteins are involved in repairing the DNA damage caused by many DNA-binding drugs commonly used in cancer treatment, such as nitrogen mustard, cisplatin, or mitomycin C (36). As a consequence, defects in the NER repair system usually increase drug sensitivity (1, 37). The widely reported finding that defects in NER decrease the sensitivity to trabectedin in both Chinese hamster ovary (7) and human cell lines (9) is somewhat paradoxical, whereas the proposal that trabectedin causes DNA breaks remains controversial (8, 9). By analyzing the sensitivity to trabectedin of a panel of NER mutants, we now show that *rad13* mutant cells are much more resistant to trabectedin than the wild-type strain, in good agreement with previous results. This mutant is more resistant than strains deficient in the endonucleases that cut on the 5′ side of the lesion, Swi10 and Rad16, which are orthologues of ERCC1 and XPF, respectively (Fig. 3). This result indicates that although the three endonucleases could play a role in the cell-killing mechanism induced by trabectedin, Rad13 is the most important one. In the absence of this structure-specific endonuclease, the cells underwent much less DNA damage (as measured by the requirement for Rad51, cell cycle delay, and Chk1 activation) and survived much better than the wild-type cells exposed to the drug (Fig. 4). In contrast, increasing levels of Rad13 led to a higher sensitivity to the drug (Fig. 3C). However, the finding that *rad13E779A* nuclease-deficient cells were not resistant (Fig. 5C) clearly indicates that the ability of Rad13 to produce SSBs is not required for the DNA damage induced by trabectedin, in contrast to a previous proposal (9). Instead, we found that it was the COOH-terminal region of the protein that confers resistance to trabectedin (Fig. 5) and—more specifically—part of its DNA-binding domain, which is highly homologous to one of the several DNA-binding domains described for the nuclease FEN-1 (ref. 32; Fig. 5). By homology modeling a Rad13/DNA-trabectedin ternary complex, we found that Arg961 (positionally and functionally

equivalent to Arg314 of FEN-1) was likely to contribute to the stabilization of the Rad13/DNA-trabectedin complex (Fig. 6*B*). In agreement with this hypothesis, an *S. pombe* strain carrying a R961A point mutation in *rad13* that did not affect its nuclease activity (Fig. 5*C*, plate + MMS and plate + 4NQO, *lane 7*) was found to be strongly resistant to the drug (Fig. 5*C*).

The formation of a putative Rad13/DNA-trabectedin cytotoxic ternary complex is consistent with earlier proposals that a protein/DNA-trabectedin intermediate in the NER processing of trabectedin-DNA adducts could be trapped and give rise to the formation of cytotoxic complexes (17, 38). DNA repair inhibition, rather than excision of the lesion, due to direct immobilization of NER factors by another type of adduct, has also been reported (39). However, the formation of other complexes between one or more DNA-trabectedin adducts and DNA repair proteins other than Rad13 cannot be ruled out.

Role of HR in the repair of the DNA damage caused by trabectedin. DSBs are serious DNA lesions, and if not repaired properly, may lead to important DNA aberrations. Two main pathways repair DSBs in eukaryotic cells: HR and nonhomologous end joining. HR is carried out by the *RAD52* group of genes (40). Mutation of any of these genes results in sensitivity to DSB-inducing agents.

Here, we show the extraordinary sensitivity to trabectedin (Fig. 3) of deletion mutants in the *RAD52* epistasis group. Because the proteins encoded by these genes are responsible for most DSB repair in eukaryotic cells, this finding can be taken as a clear indication that the drug could give rise (directly or indirectly) to DSBs. These results are in agreement with previous reports showing that trabectedin was more effective in cells lacking DNA-dependent protein kinase (involved in nonhomologous end joining). The fact that the absence of *rad13* partially rescued the great sensitivity to trabectedin of *rad51Δ* cells (Fig. 4*D*) indicates that Rad13 is somehow involved in the induction of DSBs, which could be an indirect effect like the one described for the simple alkylating agent MMS (41, 42). HR can also be induced by spontaneous SSBs probably induced by collapsed replication forks during normal DNA replication (43). Against the possibility that, in the absence of a proficient NER system (*rad13Δ*), other repair systems might be activated to compensate for this absence, thereby accounting for the better survival of *rad51Δ rad13Δ* cells, is the finding that the double mutant *rad51Δ rad13Δ* is more sensitive to MMS than the single *rad51Δ* mutant (44). This indicates that, at least in the case of MMS, no additional repair system compensates for the lack of a proficient NER.

Model for the mechanism of action of trabectedin in eukaryotic cells and relevance to cancer. Taking together the results reported here and others published in the literature, we suggest the following sequence of events for the action of trabectedin in eukaryotic cells: (*a*) trabectedin binds covalently to the DNA minor groove and the adduct is recognized by the NER system; (*b*) the recruited Rad13 (XPG) protein binds to DNA and simultaneously interacts with the minor groove-bound drug by means of Arg961; (*c*) the proteins making up the Swi10-Rad16 (ERCC1-XPF) complex are the last NER factors to arrive and, together with proteins from other DNA repair pathways that try to correct the DNA lesions, are hijacked at the sites of damage, creating stronger cytotoxic complexes; (*d*) during S phase, these complexes give rise to DNA lesions that need to be repaired by HR (e.g., DSBs) so that HR-proficient cells can repair the damage, whereas those defective in one or more HR proteins, a common observation in several solid tumors (40), will be especially sensitive to the action of the drug. In view of this likely scenario, our results may have important implications for the optimal use of trabectedin in cancer therapy because patients harboring tumor cells with proficient NER and deficient HR systems would be expected to respond best to the treatment. This hypothesis is currently being tested in clinical trials.

Acknowledgments

References

1. D'Incalci M, Erba E, Damia G, et al. Unique features of the mode of action of ET-743. Oncologist 2002;7:210–6.
2. Demetri GD. ET-743: the US experience in sarcomas of soft tissues. Anticancer Drugs 2002;13:S7–9.
3. D'Incalci M, Jimeno J. Preclinical and clinical results with the natural marine product ET-743. Expert Opin Investig Drugs 2003;12:1843–53.
4. Le Cesne A, Blay JY, Judson I, et al. Phase II study of ET-743 in advanced soft tissue sarcomas: a European Organisation for the Research and Treatment of Cancer (EORTC) soft tissue and bone sarcoma group trial. J Clin Oncol 2005;23:576–84.
5. Pommier Y, Kohlhagen G, Bailly C, Waring M, Mazumder A, Kohn KW. DNA sequence- and structure-selective alkylation of guanine N2 in the DNA minor groove by ecteinascidin 743, a potent antitumor compound from the Caribbean tunicate *Ecteinascidia turbinata*. Biochemistry 1996;35:13303–9.
6. Moore SF II, Hurley LH. NMR-based model of an ecteinascidin 743-DNA adduct. J Am Chem Soc 1997;119:5475–6.
7. Damia G, Silvestri S, Carrassa L, et al. Unique pattern of ET-743 activity in different cellular systems with defined deficiencies in DNA-repair pathways. Int J Cancer 2001;92:583–8.
8. Erba E, Bergamaschi D, Bassano L, et al. Ecteinascidin-743 (ET-743), a natural marine compound, with a unique mechanism of action. Eur J Cancer 2001;37:97–105.
9. Takebayashi Y, Pourquier P, Zimonjic DB, et al. Antiproliferative activity of ecteinascidin 743 is dependent upon transcription-coupled nucleotide-excision repair. Nat Med 2001;7:961–6.
10. Moreno S, Klar A, Nurse P. Molecular genetic analysis of fission yeast *Schizosaccharomyces pombe*. Methods Enzymol 1991;194:795–823.
11. Foiani M, Marini F, Gamba D, Lucchini G, Plevani P. The B subunit of the DNA polymerase α-primase complex in *Saccharomyces cerevisiae* executes an essential function at the initial stage of DNA replication. Mol Cell Biol 1994;14:923–33.
12. Zewail-Foote M, Hurley LH. Ecteinascidin 743: a minor groove alkylator that bends DNA toward the major groove. J Med Chem 1999;42:2493–7.
13. Carr AM. DNA structure dependent checkpoints as regulators of DNA repair. DNA Repair (Amst) 2002;1:983–94.
14. Lindsay HD, Griffiths DJ, Edwards RJ, et al. S-phase-specific activation of Cds1 kinase defines a subpathway of the checkpoint response in *Schizosaccharomyces pombe*. Genes Dev 1998;12:382–95.
15. Capasso H, Palermo C, Wan S, et al. Phosphorylation activates Chk1 and is required for checkpoint-mediated cell cycle arrest. J Cell Sci 2002;115:4555–64.
16. Lambert S, Mason SJ, Barber LJ, et al. *Schizosaccharomyces pombe* checkpoint response to DNA interstrand cross-links. Mol Cell Biol 2003;23:4728–37.
17. Soares DG, Poletto NP, Bonatto D, Salvador M, Schwartsmann G, Henriques JA. Low cytotoxicity of ecteinascidin 743 in yeast lacking the major endonucleolytic enzymes of base and nucleotide excision repair pathways. Biochem Pharmacol 2005;70:59–69.
18. de Laat WL, Jaspers NG, Hoeijmakers JH. Molecular mechanism of nucleotide excision repair. Genes Dev 1999;13:768–85.
19. Alleva JL, Zuo S, Hurwitz J, Doetsch PW. *In vitro* reconstitution of the *Schizosaccharomyces pombe* alternative excision repair pathway. Biochemistry 2000;39:2659–66.
20. Baumann P, Benson FE, West SC. Human Rad51 protein promotes ATP-dependent homologous pairing and strand transfer reactions *in vitro*. Cell 1996;87:757–66.
21. van den Bosch M, Zonneveld JB, Vreeken K, de Vries FA, Lohman PH, Pastink A. Differential expression and

requirements for *Schizosaccharomyces pombe* RAD52 homologs in DNA repair and recombination. Nucleic Acids Res 2002;30:1316–24.

22. Muris DF, Vreeken K, Carr AM, et al. Isolation of the *Schizosaccharomyces pombe* RAD54 homologue, rhp54+, a gene involved in the repair of radiation damage and replication fidelity. J Cell Sci 1996;109:73–81.

23. Van Komen S, Petukhova G, Sigurdsson S, Stratton S, Sung P. Superhelicity-driven homologous DNA pairing by yeast recombination factors Rad51 and Rad54. Mol Cell 2000;6:563–72.

24. Lieber MR. The FEN-1 family of structure-specific nucleases in eukaryotic DNA replication, recombination and repair. Bioessays 1997;19:233–40.

25. Shen B, Nolan JP, Sklar LA, Park MS. Functional analysis of point mutations in human flap endonuclease-1 active site. Nucleic Acids Res 1997;25:3332–8.

26. Wakasugi M, Reardon JT, Sancar A. The non-catalytic function of XPG protein during dual incision in human nucleotide excision repair. J Biol Chem 1997; 272:16030–4.

27. Xiao W, Chow BL. Synergism between yeast nucleotide and base excision repair pathways in the protection against DNA methylation damage. Curr Genet 1998;33: 92–9.

28. Lee SK, Yu SL, Prakash L, Prakash S. Requirement of yeast RAD2, a homolog of human XPG gene, for efficient RNA polymerase II transcription. implications for Cockayne syndrome. Cell 2002;109:823–34.

29. Shiomi N, Kito S, Oyama M, et al. Identification of the XPG region that causes the onset of Cockayne syndrome by using Xpg mutant mice generated by the cDNA-mediated knock-in method. Mol Cell Biol 2004;24: 3712–9.

30. Knauf JA, Pendergrass SH, Marrone BL, Strniste GF, MacInnes MA, Park MS. Multiple nuclear localization signals in XPG nuclease. Mutat Res 1996;363:67–75.

31. Gary R, Ludwig DL, Cornelius HL, MacInnes MA, Park MS. The DNA repair endonuclease XPG binds to proliferating cell nuclear antigen (PCNA) and shares sequence elements with the PCNA-binding regions of FEN-1 and cyclin-dependent kinase inhibitor p21. J Biol Chem 1997;272:24522–9.

32. Chapados BR, Hosfield DJ, Han S, et al. Structural basis for FEN-1 substrate specificity and PCNA-mediated activation in DNA replication and repair. Cell 2004;116:39–50.

33. Broggini M, Coley HM, Mongelli N, et al. DNA sequence-specific adenine alkylation by the novel antitumor drug tallimustine (FCE 24517), a benzoyl nitrogen mustard derivative of distamycin. Nucleic Acids Res 1995;23:81–7.

34. Gajate C, An F, Mollinedo F. Differential cytostatic and apoptotic effects of ecteinascidin-743 in cancer cells. Transcription-dependent cell cycle arrest and transcription-independent JNK and mitochondrial mediated apoptosis. J Biol Chem 2002;277:41580–9.

35. Minuzzo M, Marchini S, Broggini M, Faircloth G, D'Incalci M, Mantovani R. Interference of transcriptional activation by the antineoplastic drug ecteinascidin-743. Proc Natl Acad Sci U S A 2000;97:6780–4.

36. Beljanski V, Marzilli LG, Doetsch PW. DNA damage-processing pathways involved in the eukaryotic cellular response to anticancer DNA cross-linking drugs. Mol Pharmacol 2004;65:1496–506.

37. Furuta T, Ueda T, Aune G, Sarasin A, Kraemer KH, Pommier Y. Transcription-coupled nucleotide excision repair as a determinant of cisplatin sensitivity of human cells. Cancer Res 2002;62:4899–902.

38. Zewail-Foote M, Li VS, Kohn H, Bearss D, Guzman M, Hurley LH. The inefficiency of incisions of ecteinascidin 743-DNA adducts by the UvrABC nuclease and the unique structural feature of the DNA adducts can be used to explain the repair-dependent toxicities of this antitumor agent. Chem Biol 2001;8:1033–49.

39. Buterin T, Hess MT, Gunz D, Geacintov NE, Mullenders LH, Naegeli H. Trapping of DNA nucleotide excision repair factors by nonrepairable carcinogen adducts. Cancer Res 2002;62:4229–35.

40. West SC. Molecular views of recombination proteins and their control. Nat Rev Mol Cell Biol 2003;4:435–45.

41. Tercero JA, Diffley JF. Regulation of DNA replication fork progression through damaged DNA by the Mec1/Rad53 checkpoint. Nature 2001;412:553–7.

42. Lopes M, Cotta-Ramusino C, Pellicioli A, et al. The DNA replication checkpoint response stabilizes stalled replication forks. Nature 2001;412:557–61.

43. Saleh-Gohari N, Bryant HE, Schultz N, Parker KM, Cassel TN, Helleday T. Spontaneous homologous recombination is induced by collapsed replication forks that are caused by endogenous DNA single-strand breaks. Mol Cell Biol 2005;25:7158–69.

44. Memisoglu A, Samson L. Contribution of base excision repair, nucleotide excision repair, and DNA recombination to alkylation resistance of the fission yeast *Schizosaccharomyces pombe*. J Bacteriol 2000;182: 2104–12.